ISBN: 978-3-95450-230-1 ISSN: 2673-5350 doi:10.18429/JACoW-IBIC2021-MOPP35

COMMISSIONING AND RESULTS OF SPIRAL2 BPMs

C. Jamet, P. Legallois, GANIL, Caen, France

Abstract

Construction of a new accelerator is always an opportunity to face challenges and make new developments. The BPM diagnostics installed in the SPIRAL2 linac and the associated instrumentation are part of these developments. BPM instrumentations are, of course, used to measure positions and phases of ion beams but also transverse shapes, called ellipticity, as well as the beam velocity. Specifications involve knowing and calculating the sensitivities in position and in ellipticity as a function of the beam velocities. These impose small amplitude differences between channels, which require precise calibration of electronics. This paper describes the modelling and analysis of the BPM behaviour according to the beam velocity, the technical solutions, modifications and improvements. An analysis of the results and evolutions in progress are also presented.

INTRODUCTION

The SPIRAL2 accelerator is a new facility built on the GANIL site at Caen in France. The first ECR ion source produce ion beams, the second proton and deuteron beams. A CW RFQ accelerates beams with A/Q ≤ 3 at energy of 0.74 MeV/A (ß ≈ 0.04). The injector commissioning took place from end 2015 to 2019 [1] with the qualification of the diagnostic monitors [2].

A high power CW superconducting linac produces up to 5 mA beams with a maximum energy of 33 MeV for protons and 20 MeV/A for deuterons. The linac is composed of 19 cryomodules, 12 with one ß = 0.07 cavity and 7 with 2 ß = 0.12 cavities. The HEBT lines distribute the linac beam to a beam Dump, to NFS (Neutron For Science) or to S3 (Super Separator Spectrometer) experimental rooms [3]. A proton beam at 33 MeV, 5 mA and a power of 16 kW was produced in 2020.

BPMs are installed inside quadrupoles in the warm sections of the linac between cryomodules. BPMs are composed of 4 squared electrodes with a radius of 24 mm, a length of 39 mm and an electrode angle of 60°.

LINAC CAVITY TUNING

The ß values in the linac are from 0.04 up to 0.26 for the 33 MeV proton beam. The first cavity tuning step consists to tune the phase and amplitude of the cavities one by one at low beam power, the downstream cavities being detuned to avoid beam energy changes. Three BPM phase measurements, one before and two after the cavity to tune, allow to measure the beam velocity. After aligning the beam using the BPM positions, the cavity phase is scanned over 360° to find the buncher phase. Comparisons with theoretical values allow to compute the cavity voltage and phase to be applied. The second step is to match the beam to the linac with quadrupole tunings in the MEBT by an iterative process. The matching method uses the ellipticity values given by the BPMs. The last step is to gradually increase the beam power while monitoring beam losses.

BPM SPECIFICATIONS

The BPM specifications to tune the SC linac cavities are given in (Table 1).

Table 1: BPM Specifications

Parameter	Resolution	Range
Position	+/- 150 µm	+/-20 mm
Phase	+/-0.5 deg.	+/-180 deg.
Ellipticity	+/-20 % or +/- 1.2 mm^2	

At low velocities, sensitivities in position and ellipticity are function of the beam beta and the frequency harmonic [4]. One of our objectives was to find a formula to calculate the ellipticity sensitivity correction.

BPM MODEL

Equations

Beam bunches generate a periodical beam current represented by a Fourier series [4].

$$I_b(t) = \langle I_b \rangle \left[1 + 2\sum_{n=1}^{\infty} A_n cos(n\omega_0 t + \phi_n) \right]$$

- I_b the beam intensity
- $<I_b>$ the average beam intensity
- A_n the Fourier component amplitudes
- ω_0 the fundamental pulsation
- ϕ_n the Fourier component phases

The wall current density i_w, at frequency $n\omega_0/2pi$, induced by a pencil beam on the conducting cylindrical tube is given by the equation [5]:

$$i_w(n\omega_0, r, \theta, \phi_w) = \frac{A_n \langle I_b \rangle}{\pi a} \left[\frac{I_0(gr)}{I_0(ga)} + 2\sum_{m=1}^{\infty} \frac{I_m(gr)}{I_m(ga)} cos\Big(m(\phi_w - \theta)\Big) \right]$$

- r the beam radius
- a the radius of the tube
- ϕ_ω the position angle on the cylindrical tube
- θ the beam angle
- $I_m()$ the modified Bessel function of order m

With

$$g = \frac{n\omega_0}{\beta\gamma c} = \frac{n\omega_0\sqrt{1-\beta^2}}{\beta c}$$

- λ the wave length
- γ the Lorentz factor
- $n\omega_0$ the pulsation

ISBN: 978-3-95450-230-1 ISSN: 2673-5350 doi:10.18429/JACoW-IBIC2021-MOPP35

With a Gaussian shape for the bunch longitudinal distribution, the instantaneous beam current is:

$$I_b(t) = \frac{\langle I_b \rangle}{\sqrt{2\pi}\sigma_{tp}} e^{-\frac{(t)^2}{2\sigma_{tp}^2}}$$

- $<I_b>$ the average beam intensity
- σ_{tp} the RMS length in time of the beam pulse

The Fourier component amplitudes A_n are:

$$A_n = e^{\left[\frac{-n^2\omega_0^2\sigma_{tp}^2}{2}\right]}$$

The wall current through the electrodes corresponds to the integration of the density on the electrode angles.

$$I_{w(r,l,u,d)}(n\omega_0, r, \theta) = \int_{angle_{elec-}}^{angle_{elec+}} i_w a d\phi_w$$

Wall current equations are simplified by taking only the Bessel coefficients of order 2 and with gr << 1. The formulas are then written for a large Gaussian beam.

$$I_{w(R,L,U,D)} = \int_{-\infty}^{\infty}\int_{-\infty}^{\infty} \frac{1}{\sigma_x\sqrt{2\pi}} \frac{1}{\sigma_y\sqrt{2\pi}} I_{w(r,l,u,d)}(x, y, X_0, Y_0) e^{\frac{-x^2}{2\sigma_x^2}} e^{\frac{-y^2}{2\sigma_y^2}} dxdy$$

$$I_{wR,L} = \frac{A_n\langle I_b \rangle}{\pi}\left[\frac{\phi_0}{I_0(ga)} \pm \frac{2g}{I_1(ga)} sin(\frac{\phi_0}{2}) X_0 + \frac{g^2 sin(\phi_0)}{4I_2(ga)}\left((X_0^2 - Y_0^2) + (\sigma_x^2 - \sigma_y^2)\right)\right]$$

$$I_{wU,D} = \frac{A_n\langle I_b \rangle}{\pi}\left[\frac{\phi_0}{I_0(ga)} \pm \frac{2g}{I_1(ga)} sin(\frac{\phi_0}{2}) Y_0 - \frac{g^2 sin(\phi_0)}{4I_2(ga)}\left((X_0^2 - Y_0^2) + (\sigma_x^2 - \sigma_y^2)\right)\right]$$

- A_n the Fourier component amplitudes
- ϕ_0 the electrode angular width
- X_0, Y_0 the horizontal and vertical positions (mm)
- ϕ_0 the angle of electrodes (radian)
- σ_x ,σ_y The horizontal and vertical RMS sizes (mm)
- I_0, I_1, I_2: Modified Bessel functions of order 0,1,2

The positions and ellipticity with a beam of transverse Gaussian distributions are defined taking into account the sensibility corrections.

$$X = \frac{K}{1+G} \frac{(I_{wR} - I_{wL})}{(I_{wR} + I_{wL} + I_{wU} + I_{wD})}$$

$$Y = \frac{K}{1+G} \frac{(I_{wU} - I_{wD})}{(I_{wR} + I_{wL} + I_{wU} + I_{wD})}$$

K, the position sensitivity, is function of the mechanical dimensions.

$$K = \frac{\phi_0 a}{2sin(\frac{\phi_0}{2})}$$

- ϕ_0 the angle of electrodes (radian)
- a the radius of the tube

Ellipticity is defined as $\sigma_x^2 - \sigma_y^2$ where σ_x and σ_y are the standard deviation of the transverse sizes of the beam. Ellipticity is calculated from the formula:

$$Ell = (\sigma_x^2 - \sigma_y^2) = \frac{S}{1+G_E} \frac{(I_{wR} + I_{wL}) - (I_{wU} + I_{wD})}{(I_{wR} + I_{wL} + I_{wU} + I_{wD})} - (X^2 - Y^2)$$

S, the ellipticity sensitivity, is also function of the radius and the electrode angle.

$$S = \frac{a^2\phi_0}{2sin(\phi_0)}$$

For SPIRAL2 BPMs, K = 25.1 mm, S = 348 mm^2

For gr << 1, the simplified equations of G, the correction coefficient of the position sensitivity, and GE the correction coefficient of the ellipticity sensitivity are:

$$1+G \approx \frac{I_0(ga)}{I_1(ga)} \frac{ga}{2} \qquad (1+G_E) \approx \frac{I_0(ga)(ga)^2}{8I_2(ga)}$$

Values of the corrected sensitivities in function of different beta in the linac are shown on the Table 2.

Table 2: SPIRAL2 BPM Corrected Sensitivities

beta	Kh1 (mm)	Kh2 (mm)	Sh1 (mm^2)	Sh2 (mm^2)
0.04	21.8	16.6	290	194
0.08	24.2	22	331	290
0.12	24.7	23.6	341	320
0.26	25.0	24.8	347	342

From the wall current, the wall density charges are calculated at a given $n\omega_0$.

$$\lambda_{R,L} \approx \frac{A_n < I_b >}{\pi\beta c}\left[\frac{\phi_0}{I_0(ga)} \pm \frac{2g}{I_1(ga)} sin(\frac{\phi_0}{2}) X_0 + \frac{g^2 sin(\phi_0)}{4I_2(ga)}\left((X_0^2 - Y_0^2) + (\sigma_x^2 - \sigma_y^2)\right)\right]$$

$$\lambda_{U,D} \approx \frac{A_n < I_b >}{\pi\beta c}\left[\frac{\phi_0}{I_0(ga)} \pm \frac{2g}{I_1(ga)} sin(\frac{\phi_0}{2}) Y_0 - \frac{g^2 sin(\phi_0)}{4I_2(ga)}\left((X_0^2 - Y_0^2) + (\sigma_x^2 - \sigma_y^2)\right)\right]$$

The integrations of the charge density over the electrode length can be written as the product of convolution of the charge density with a Heaviside step function at the electrode length.

$$Q_{elec}(t) = \beta c\lambda \otimes \mathcal{H}(t)$$

In the frequency domain, the Fourier transform of the charge is the product of the Fourier Transform of the charge density by the step function.

$$\tilde{Q}_{elec}(f) = \beta c\tilde{\lambda} \times \tilde{\mathcal{H}}(f)$$

The Fourier transform of the periodical charge signal is then:

$$\tilde{Q}_{elec}(f) = L_{elec} sinc(\pi\frac{L_{elec}}{\beta c} f)\lambda_{R,L,U,D}$$

The electrode intensity, the derivation of the charge, generates amplitude on Z_{rc}, the impedance of the resistor R in parallel with the electrode capacitance C. Electrode voltages are defined by:

$$\tilde{U}_{elec}(f) = 2\pi i f Z_{RC} sinc(\pi\frac{L_{elec}}{\beta c} f) L_{elec}\lambda_{R,L,U,D}$$

ISBN: 978-3-95450-230-1 ISSN: 2673-5350 doi:10.18429/JACoW-IBIC2021-MOPP35

BPM electronic modules measure the electrode amplitudes at the first (h1, F_{acc} = 88.0525 MHz) and second (h2, 176.105 MHz) harmonics. The h1 and h2 electrode amplitudes are obtained from the Fourier Transform.

$$V_{h1_{eff}-(elec-R,L,U,D)} = \sqrt{2}|Z_{RC_{h1}}|I_{w(R,L,U,D)}sin(\pi\frac{L_{elec}}{L_{acc}})$$

$$V_{h2_{eff}-(elec-R,L,U,D)} = \sqrt{2}|Z_{RC_{h2}}|I_{w(R,L,U,D)}sin(2\pi\frac{L_{elec}}{L_{acc}})$$

$$|Z_{RC_{h1}}| = \frac{R}{\sqrt{1+(2\pi F_{acc}RC)^2}} \qquad |Z_{RC_{h2}}| = \frac{R}{\sqrt{1+(4\pi F_{acc}RC)^2}}$$

In this model, equations are function of σ_{tp} the standard deviation of the bunch in time (Fourier component terms "A_n"), the electric field enlargement is taken into account by the Bessel coefficients.

A vector summation of the 4 electrode signals is calculated by the electronic boards to give a vector-sum amplitude and phase. The sum of the charge density is proportional to the beam intensity.

$$I_{wR} + I_{wL} + I_{wU} + I_{wD} = \frac{4}{3}\frac{\langle I_b\rangle}{I_0(ga)}A_n$$

Considering that the phases of the 4 BPM signals are identical, the RMS amplitudes of the vector-sum h1 and h2 are:

$$V_{VS-h1_{eff}} = \frac{4\sqrt{2}}{3}|Z_{RC_{h1}}|sin(\pi\frac{L_{elec}}{L_{acc}})\frac{\langle I_b\rangle}{I_0(g_{h1}a)}e^{-2\pi^2\sigma_{tp}^2F_{acc}^2}$$

$$V_{VS-h2_{eff}} = \frac{4\sqrt{2}}{3}|Z_{RC_{h2}}|sin(2\pi\frac{L_{elec}}{L_{acc}})\frac{\langle I_b\rangle}{I_0(g_{h2}a)}e^{-8\pi^2\sigma_{tp}^2F_{acc}^2}$$

With

$$L_{acc} = \frac{\beta c}{F_{acc}}$$

The bunch length is calculated from the ratio of h1 and h2 vector-sum amplitudes.

$$\sigma_{tp} = \frac{1}{\sqrt{6}\pi F_{acc}}\sqrt{ln[2\frac{|Z_{RC_{h2}}|}{|Z_{RC_{h1}}|}cos(\pi\frac{L_{elec}}{L_{acc}})\frac{I_0(g_{h1}a)}{I_0(g_{h2}a)}(\frac{V_{VS-h1_{eff}}}{V_{VS-h2_{eff}}})]}$$

BPM INSTRUMENTATION

BPM Electronic Boards

BPM electronic boards were designed and realized in the framework of collaboration between the BARC Indian laboratory and GANIL. The BPM system consists of a set of two VME64x based 6U boards, an Analog and Digital boards. BPM systems process signals either at the 88.0525 MHz fundamental frequency or at the second harmonic for both amplitude and phase measurements. Horizontal and vertical positions, ellipticity, amplitude and phase of the vector-sum are calculated from both h1 and h2 measurements. The input signal range is between -20 and -65 dBm with a variable gain from 13.5 to 60 dB.

The design of the BPM system is based on the scheme of auto-gain equalization using offset tone. In this scheme, the gain of the different channels is equalized with respect to the injected offset tone. The scheme consists to digitally generate an amplitude and phase stable offset tone having a small frequency shift with respect to the RF reference. This offset tone is added to each of the four incoming signals [6].

Calibration and Stabilisations

In order to obtain the required resolutions, 2 solutions were implemented in the electronic process, a very precise calibration and stabilizations of the 4 gains and phases. The calibration is used to correct the gain and phase deviations of signals and offset tone on the 4 channels at h1 and h2. Calibration signals around -20 dBm are send successively to the 4 channels. Correction coefficients are next memorized in a file used to initialize BPM boards during startup. Gain and phase stabilizations were designed to correct gain and phase deviations over the entire operating range. Deviations come from drift effects like temperature and from gain and phase differences of attenuators.

Calibration Results

After the calibration, tests are carried out with a generator to verify the results, maximum shifts in amplitudes between the four channels in function of the level (Fig. 1), shifts in phase (Fig. 2) are also measured.

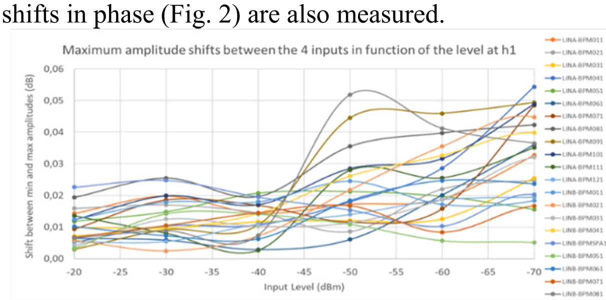

Figure 1: Max. amplitude shifts between the 4 channels.

Amplitude shifts generates +/- 0.03 mm position and +/- 0.5 mm2 ellipticity variations in function of the level from -20 dBm to -70 dBm. The maximum phase shift between channels is limited to 0.5° in this level range and the phase difference between boards is lower than +/- 0.5°.

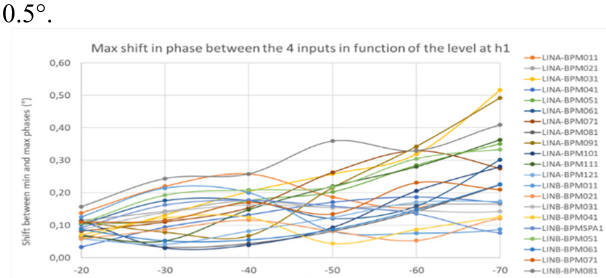

Figure 2: Max. phase shifts between the 4 channels.

MODIFICATIONS AND IMPROVEMENTS

Important precautions have been taken regarding the choice and installation of cables. After tests, the ACOME M5333Z cable was chosen for the BPMs to electronic cabinet connexions. Attenuations are 0.85 dB at h1 and 1.4 dB at h2 for cable lengths of 23 m +/- 10 mm. The 80

ISBN: 978-3-95450-230-1 ISSN: 2673-5350 doi:10.18429/JACoW-IBIC2021-MOPP35

cables were grouped by 4 in function of their phase before installation. The lengths of small cables inside the 2 BPM cabinets were adjusted so that the overall phase of the cables is very close (+/- 0.4° shifts at 88.0525 MHz).

The BPM commissioning on the D-Plate, from 2016 to 2018, allows to learn how to use, calibrate, qualify and modify the BPM electronics [7]. The main modifications were to add shielding on the analog cards to reduce the coupling between certain channels and to limit the EMC disturbances on cabinets and cables.

The validation of position and ellipticity measurements with beams was more complicated due to difficulties to compare BPM measurements with other diagnostics and to know very precisely the beam characteristics at the BPM positions. However, the comparisons between h1 and h2 allowed us to understand that the differences in impedance matching of the 4 electronic board inputs disturbed the amplitude measurements. The required ellipticity measurement accuracy imposes severe constraints in terms of gain on the 4 channels (+/- 0.03 dB for +/- 1.2 mm^2). Early 2020, a 50 Ω matching was added on each BPM cable output. A small cable was also added on each output, with a length adjusted to have an open circuit as well as a SMA T adapter and a 50 Ω. The beam measurements are now made under the same matching conditions as the calibration.

RESULTS WITH BEAMS

In 2020, a 4.15 mA proton beam at 33 MeV, generated the BPM signals shown by Fig. 3. The h1 amplitudes (purple curve) gradually decrease when the velocity increase. The h2 amplitudes (orange curve) reach a maximum for a beta around.

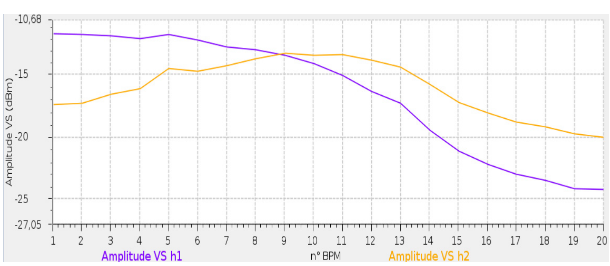

Figure 3: h1 and h2 amplitudes from the 20 BPMs.

Position and ellipticity values show a good agreement between h1 and h2 measurements and confirm the correctness of the formulas of the sensitivity coefficients. (Figs. 4 and 5).

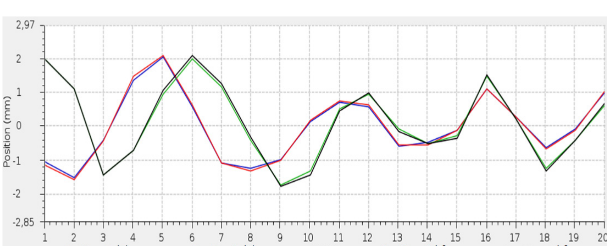

Figure 4: h1 and h2 positions from the 20 BPMs.

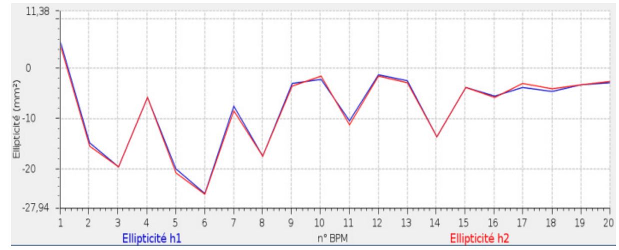

Figure 5: h1 and h2 ellipticities from the 20 BPMs.

Amplitude calculations taking the measured beam intensity with an ACCT and the bunch lengths given by the TraceWin code [8] are compared with the measured h1 and h2 vector-sum (VS) amplitudes. The calculated and measured curves are relatively close and validate the VS amplitude equations (Fig. 6).

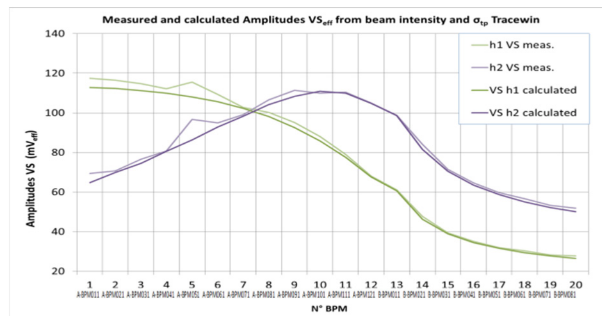

Figure 6: Measured and calculated VS amplitudes.

Bunch length calculations from the h1 and h2 vector-sum request precise measurements of the cable losses at both harmonics. Length values are actually very sensitives to low amplitudes variations, few % of differences on the h1/h2 ratio can generate important errors. Comparisons between calculated values from h1/h2 and length values from the TraceWin code did not give satisfactory results. More measurements will be done with different beams to better understand and improve this important measurement for linac tuning.

Early 2021, an improved cavity tuning procedure using beam energy measurements from the BPMs was tested. A new calibration procedure, taking into account the phase drift from BPM outputs, was applied to correct these phase shifts and have the same phase reference for the 20 BPM monitors.

In July 2021, with a helium beam at 40 MeV, beam energies were measured using the Time of Flight monitor (ToF) located at the linac exit to check the BPM measurements. Figure 7 shows that from cavity 12 the energy differences are relatively small, this validated the BPM phase accuracies and the calibration procedure.

ISBN: 978-3-95450-230-1 ISSN: 2673-5350 doi:10.18429/JACoW-IBIC2021-MOPP35

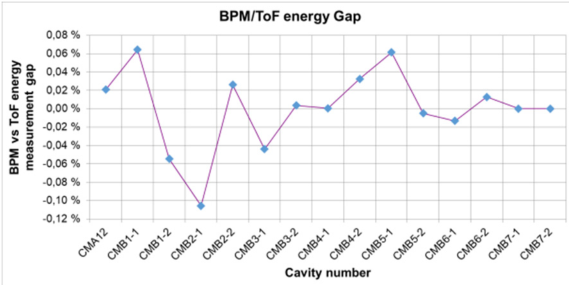

Figure 7: Energy differences between BPMs and ToF.

CONCLUSIONS

After various optimizations, the BPM systems meet the requirements and allow an optimal setting of the linac. The position and ellipticity sensitivities are calculated and applied for each new beam according to the theoretical velocity parameters. The calibration and stabilization systems allow to obtain a very good precision, big thanks to the BARC team which conceived and provided these systems. The next actions concern the development of a "Post-Mortem" system of data storage with an acquisition rate of 10 µs, an improvement of the bunch length measurements, an automation of the calibrations and an increase of the sensitivity towards the very low levels.

REFERENCES

[1] R. Ferdinand *et al.*, “Final Results of the SPIRAL2 Injector Commissioning”, in *Proc. 10th Int. Particle Accelerator Conf. (IPAC'19)*, Melbourne, Australia, May 2019, pp. 848-851. doi:10.18429/JACoW-IPAC2019-MOPTS006

[2] C. Jamet *et al.*, “SPIRAL2 Diagnostic qualifications with RFQ beams”, in *8th Int. Beam Instrumentation Conf. (IBIC’19)*, Malmö, Sweden, Sep. 2019. doi:10.18429/JACoW-IBIC2019-MOPP036

[3] P. Dolegieviez, R. Ferdinand, X. Ledoux, H. Savajols, and F. Varenne, “Status of the SPIRAL2 Project”, in *Proc. 10th Int. Particle Accelerator Conf. (IPAC'19)*, Melbourne, Australia, May 2019, pp. 844-847. doi:10.18429/JACoW-IPAC2019-MOPTS005

[4] R. E. Shafer, “Beam Position Monitor Sensitivity for Low-beta; Beams”, in *Proc. 1994 Linear Accelerator Conf. (LINAC'94)*, Tsukuba, Japan, Aug. 1994, paper TH-84, pp. 905-907.

[5] J. H Cupérus, “Monitoring of particle beam at high frequencies*”, Nuclear Instrument and Methods,* vol. 145*,* pp. 219-231, 1977.

[6] G. Joshi *et al.*, “An offset tone based gain stabilization technique for mixed-signal RF measurement systems”, *Nucl. Instr. Meth. A*, vol. 795, pp. 399-408, 2015. doi:10.1016/j.nima.2015.06.015

[7] P. Ausset *et al.*, “Operation of the Beam Position Monitor for the Spiral 2 Linac on the Test Bench of the RFQ”, in *Proc. 5th Int. Beam Instrumentation Conf. (IBIC'16)*, Barcelona, Spain, Sep. 2016, pp. 642-645. doi:10.18429/JACoW-IBIC2016-WEPG11

[8] D. Uriot and N. Pichoff, “Status of TraceWin Code”, in *Proc. 6th Int. Particle Accelerator Conf. (IPAC'15)*, Richmond, VA, USA, May 2015, pp. 92-94. doi:10.18429/JACoW-IPAC2015-MOPWA008